α and β Interfacial Structures of the iPP/PET Matrix/Fiber Systems

Xiaoli Sun,[†,‡] Huihui Li,[†] Ingo Lieberwirth,[‡] and Shouke Yan*[,†]

State Key Laboratory of Polymer Physics and Chemistry, Institute of Chemistry, The Chinese Academy of Sciences, Beijing 100080, P. R. China, and Max Planck Institute for Polymer Research, D-55128 Mainz, Germany

Received June 21, 2007; Revised Manuscript Received September 3, 2007

ABSTRACT: The interfacial structures of the iPP/PET matrix/fiber composite systems prepared by introducing the PET fiber into the iPP melt or supercooled melt were studied via optical and scanning electron microscopies. We found that unlike the iPP matrix/fiber single polymer composites prepared in the same way, where homoepitaxy induced by solid α-iPP fiber dominates the crystallization process of the iPP matrix, the iPP in iPP/PET composites displays the feature of crystallization in temperature gradient. Optical microscopy observations show that the interfacial structures of the iPP/PET composites depend strongly on the fiber introduction temperature. At higher fiber introduction temperature, e.g., over 170 °C, the crystallization of iPP takes place in its α-phase. At lower fiber introduction temperature, e.g., below 145 °C, the iPP crystallizes in its β-phase. This is different from the crystallization of iPP in iPP/PET composite under quiescent conditions, where the PET exerts only a moderate α nucleating effect toward iPP and may provide a new way for the preparation of β iPP.

Introduction

Understanding of shear-induced crystallization of semicrystalline polymers is of great importance both in the fields of polymer engineering since it is encountered in many processing approaches and of fundamental research for external flow causes orientation of molecules in a polymer melt and thus affects its overall crystallization kinetics, structure, and resultant morphology. Therefore, it has been an extremely active research topic in the past few decades. Among many others, isotactic polypropylene (iPP) has been most frequently chosen as model system since the structure of it reflects very sensitively the changes in processing parameters and depends strongly on molecular parameters such as molecular weight, molecular weight distribution, and chain branching.[1,2] Systematic rheo-optical and rheo-X-ray studies on the flow-induced crystallization of iPP indicate that shear flow enhances the crystallization rate and promotes the formation of oriented structure, even extended chain shish structure.[2−15] Moreover, it was found that crystallization from sheared or strained iPP melt encourages the crystallization of it in its β-phase.[16−20] The mechanism of its β-crystallization remains, however, a long-standing problem.

To disclose the origin of shear-induced β-crystallization of iPP, Varga et al. have adopted an elegant experimental procedure in which the shear is created via fiber pulling.[21−23] On the basis of the resultant unusual interfacial structures of iPP, the formation mechanism of shear-induced β-iPP crystallization has been discussed. They found that the β-iPP crystals grow on a thin layer of oriented α-crystals and therefore concluded that shear-induced α-row nuclei take response of the β-iPP crystal growth through a αβ growth transition. On the other hand, it was found that crystallization of iPP in temperature gradient is also in favor of the formation of β-iPP crystals.[24−26] It was reported that a kinetically favored α to β growth transition could occur during crystallization of iPP in temperature gradient, which was not related to the formation of oriented α row nuclei.[19,25]

To get more insight into the β-crystallization of iPP, our research group has utilized another experimental setup.[27−30] As shown in Figure 1, the experiments were realized by introducing the highly oriented iPP fibers into their homogeneity molten or supercooled molten matrix. Systematic studies show that β-crystallization of iPP is a nucleation-dominated process. Molecular chain or chain segment orientation in the melt plays a very important role in generating β-crystallization. It seems that there exists an orientation window of iPP molecules in the molten state, which enables the β-nucleation of iPP.[27,31] It should be pointed out that, in our experimental procedure for the iPP single polymer system, the chain orientation of iPP is mainly controlled by thermal history of the preoriented fibers. There may be also some extent of shear on the iPP matrix caused by fiber introduction.[30] To distinguish the contribution of the shear-induced part from the partially molten fiber induced crystallization and for a better comparison of our experimental procedure with the fiber pulling test adopted by Varga et al., iPP/PET matrix/fiber systems prepared by introducing the PET fiber into the iPP melt or supercooled melt were studied.

The purpose of this paper is to present the detailed interfacial morphological features of the resultant iPP/PET matrix/fiber systems as a function of fiber introduction temperature. On the basis of the results obtained, the mechanism of iPP β-crystallization was discussed.

Experimental Section

The matrix polymer used in this work was iPP, GB-2401, with melting flow index of 2.5 g/10 min, M_w of 4.4×10^5 g/mol, and melting temperature of 170 °C, produced by Yanshan Petroleum and Chemical Cor., China. The granular iPP materials were used without any further treatment. The highly oriented PET fibers with diameter of ca. 15 μm were kindly supplied by Donghua University, China. To remove the sizing agents on the fiber surface, the fibers were rinsed for 4 h in a distillation flask with acetone and then dried in a vacuum oven at 40 °C for 4 h. Thin iPP films, ca. 40 μm in thickness, were prepared by compression-molding the iPP granules at 200 °C with a pressure of 7.5×10^6 Pa. The iPP/PET matrix/fiber heterogeneity composites were produced by a procedure same as that used in the study of iPP homogeneity matrix/fiber systems.[27] As shown in Figure 1, the iPP matrix thin films were

* To whom all correspondence should be addressed: e-mail skyan@iccas.ac.cn, Tel 0086-10-82618476, Fax 0086-10-82618476.
† The Chinese Academy of Sciences.
‡ Max Planck Institute for Polymer Research.

10.1021/ma071382x CCC: $37.00
Published on Web 10/13/2007

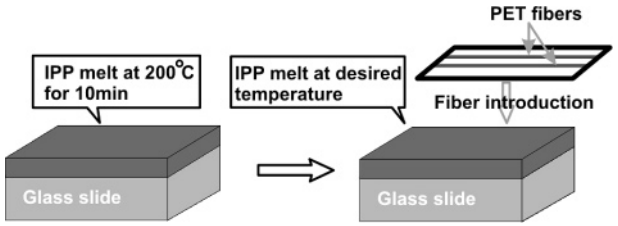

Figure 1. Sketch showing the sample preparation procedure.

first heated to 200 °C for 10 min to erase their thermal history completely and subsequently moved to a preheated hot plate, where the iPP matrix was kept in the molten or supercooled molten state at the temperature of fiber introduction. As the iPP molten thin layers reached equilibrium at the desired temperature, the PET fibers supported by a metal frame (with both ends of the PET fiber being fixed on the metal frame to avoid the shrinkage of the fiber) were introduced into the iPP matrix melts. The thus prepared fiber/matrix composites were subsequently moved to another hot plate at 130 °C for a 90 min isothermal crystallization.

For optical microscopy observation, an Olympus BH-2 optical microscope equipped with a hot stage was used in this study. The interfacial structures were viewed step by step along the whole PET fiber. All optical micrographs presented in this paper were taken under crossed polarizers.

The samples for scanning electron microscopy (SEM) study were first etched according to a procedure introduced by Bassett[32] and then sputtered with a thin layer of Pt to increase the sample stability under electron beam and enhance the contrast of the images. The PET fiber was detached from the sample during etching, which should be dissolved in permanganic agent. In this case, the structure in its vicinity remains intact. For SEM observation, a JSM-6700F field emission scanning electron microscope operated at 5 kV was used in this study.

Results

Figure 2 shows the optical micrographs of the iPP/PET matrix/fiber composite samples, which were prepared by introducing the PET fibers into the iPP matrix at temperatures of (a) 200 °C and (b) 180 °C and subsequently moved to another hot plate at 130 °C for isothermal crystallization. From Figure 2, it can be clearly seen that the interfacial morphologies of the matrix/fiber systems depend strongly on the temperature at which the fibers were put into the matrix (we termed it hereafter fiber introduction temperature). As shown in Figure 2a, if the PET fiber is introduced into the iPP matrix at 200 °C, supramolecular structures formed from individual nuclei are perceptible in the micrographs. The iPP crystals triggered by these nuclei grow individually in semispherulitic form at the beginning and meet each other soon in the lateral direction. This leads to the crystal growth direction changes gradually to the transverse direction of the PET fiber axis and forms columniform structures. Along the whole PET fiber, approximately same morphologies were observed except for a slight increase in nucleus density at both ends of the PET fiber. Moreover, it was found through selective melting test that the iPP crystals grown either from the PET fiber or in the bulk are all of α-form. On the other hand, if the fiber introduction temperature is set at 180 °C (Figure 2b), an overall increment in nucleation density of iPP by the PET fiber is seen, which results in a quick formation of regular column structure of iPP surrounding the PET fiber. Nevertheless, all the crystals observed are also composed of pure α-iPP crystals. The above observations indicate that lower fiber introduction temperature is in favor of the nucleation of iPP on the PET fiber surface. Therefore, the interfacial structures of the samples prepared at even lower fiber introduction temperatures were monitored.

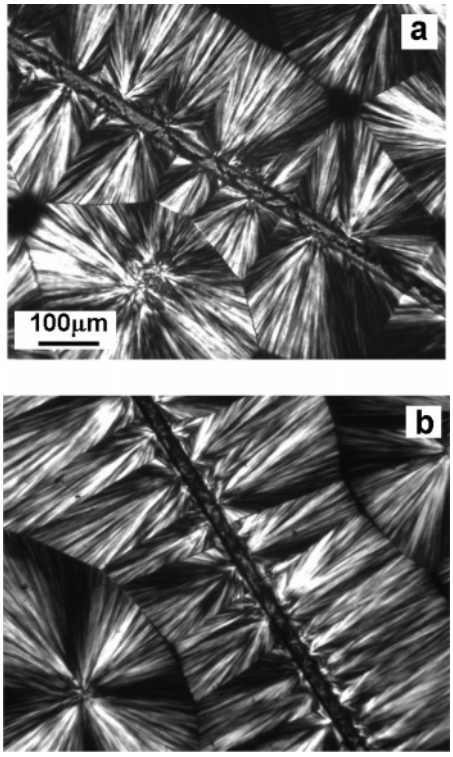

Figure 2. Optical micrographs of the iPP/PET composites, which were prepared by introducing the PET fibers into the iPP melts at (a) 200 and (b) 180 °C. After introduction of the PET fibers, the composites were moved directly to another hot plate at 130 °C and crystallized isothermally for 90 min.

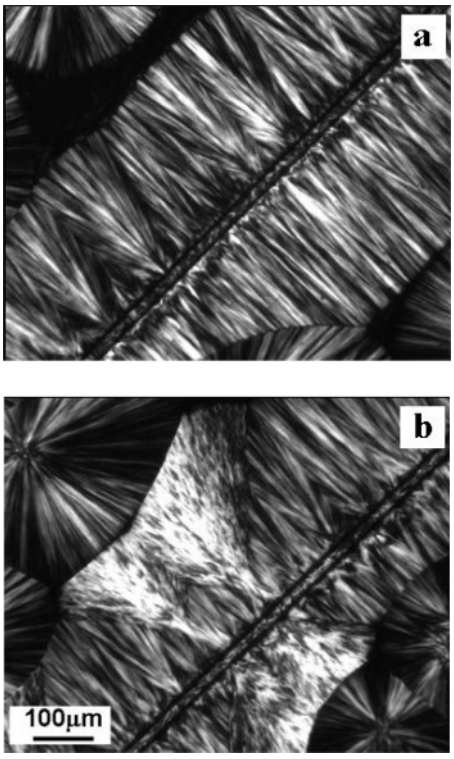

Figure 3. Optical micrographs of an iPP/PET composite, which was prepared by introducing the PET fiber into the iPP melt at 170 °C, and crystallized isothermally at 130 °C for 90 min. The pictures were taken at (a) center part of the PET fiber and (b) tips of the PET fiber.

Figure 3 presents the optical micrographs of an iPP/PET matrix/fiber composite sample, which was prepared by introducing the PET fiber into the iPP matrix at 170 °C (which is the same as the nominal melting temperature of iPP) and then

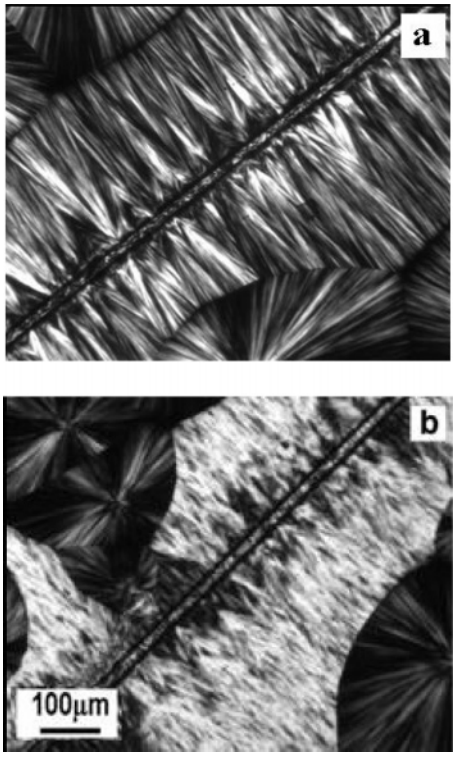

Figure 4. Optical micrographs of an iPP/PET composite, which was prepared by introducing the PET into the supercooled iPP melt at 160 °C and crystallized isothermally at 130 °C for 90 min. The pictures were taken at (a) center part of the PET fiber and (b) tips of the PET fiber.

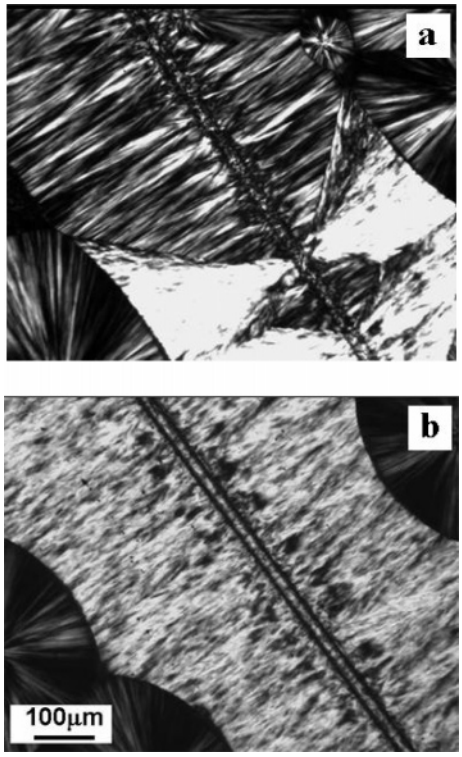

Figure 5. Optical micrographs of an iPP/PET composite, which was prepared by introducing the PET into the supercooled melt at 150 °C and crystallized isothermally at 130 °C for 90 min. The pictures were taken at (a) center part of the PET fiber and (b) tips of the PET fiber.

crystallized isothermally at 130 °C for 90 min. Now, except for the overall increase in the nucleation density, the interfacial structures of iPP at two tips of the PET fiber are somewhat different from that at the middle part of the PET fiber. In the middle part of the PET fiber, as shown in Figure 3a, well-developed columniform structures in α-modification of iPP are observed. At both ends of the PET fiber (see Figure 3b), some fan-shaped crystals inlaid in the well-defined α-iPP crystalline layers can be clearly observed. These fan-shaped crystals exhibit much stronger birefringence with respect to their surroundings and are attested to be the β-phase iPP crystals. This phenomenon is more pronounced with further decrease of the fiber introduction temperature. As an example, Figure 4 shows the optical micrographs of an iPP/PET matrix/fiber sample prepared by introducing the PET fiber into a supercooled iPP matrix at 160 °C. In the middle part of the PET fiber (Figure 4a), the interfacial morphology has a close resemblance with that shown in Figure 3a. At the end of the PET fiber (Figure 4b), the morphology is, however, quite different from that shown in Figure 3b. First of all, the amount of fan-shaped β-crystals increases tremendously. These fan-shaped β-crystals space closely and form columniform structure around the PET fiber like their α-counterparts. Moreover, the regions containing β-iPP crystals at both ends of the PET fiber are much larger than that shown in Figure 3b.

The regions containing β-iPP crystals were found to get larger and larger with decreasing fiber introduction temperature. The expansion of the β-iPP crystal regions is achieved through propagation from the fiber tip to the middle along the PET fiber axis. In other words, the window of pure α-iPP crystals in the middle part of the PET fiber reduces gradually with decreasing temperature of fiber introduction. By introducing the PET fiber into the supercooled iPP matrix at 150 °C, the window of pure α-iPP crystals becomes so small that a picture of only α-iPP column structure at present magnification is hardly recorded (see Figure 5a). In this case, well-defined column structures of β-iPP are observed all along the PET fiber apart from the center place (see Figure 5b). Henceforth, β-iPP column structures become the solely observed interfacial morphologies along the whole PET fibers with further decrease in the fiber introduction temperature. Figure 6a shows a representative optical micrograph of a sample prepared by putting the PET fiber into the iPP supercooled melt at 140 °C and then crystallized at 130 °C for 90 min. The morphologies are quite uniform along the whole PET fiber under an optical microscope. Selective melting at 160 °C tells us that the column structure is composed of purely β-iPP crystals.

Discussion

From the above experimental results, one can conclude that the interfacial morphologies of our iPP/PET matrix/fiber systems depend remarkably on the fiber introduction temperature as well as the position along the fiber axis. Lower fiber introduction temperature or at end parts of the PET fiber are found to be suitable for creating β-iPP crystals. From this point of view, the crystallization mechanism of iPP in its β-form can be discussed. In our previous work,[30] we proposed that some extent of shear on the iPP matrix directly in contact with the fiber could be created during the fiber introduction. To find out the validity of this suggestion, an experiment was performed with the PET fiber introduced into the iPP supercooled melt at 145 °C. The sample was then kept at this temperature for different times to adjust the orientation of the iPP chains or chain segments through relaxation and finally moved to another hot plate at 130 °C for isothermal crystallization. As shown in Figure 7a, by keeping the sample at 145 °C for 5 s after fiber introduction whereas before crystallization, the interfacial morphology is in principle the same as that shown in Figure

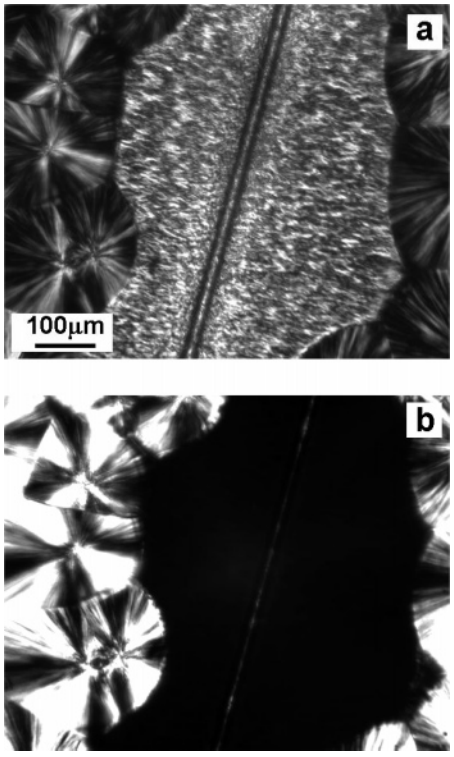

Figure 6. Optical micrographs of an iPP/PET composite, which was prepared by introducing the PET into the supercooled iPP melt at 140 °C and crystallized isothermally at 130 °C for 90 min: (a) as-prepared sample and (b) after selective melting at 160 °C for 5 min.

6a. A 30 s placement of the sample at 145 °C before isothermal crystallization, as shown in Figure 7b, leads to the formation of cylindrites rich in β-iPP crystals but with some triangular α-iPP crystals sporadically inlaid in the well-developed β-iPP column layers, as indicated by white arrows in the picture. When the sample was kept at 145 °C for 10 min, as shown in Figure 7c, even though the cylindrites are still the observed interfacial morphology, they are, however, composed of purely α-iPP crystals. From this result, it seems that there exists of varying extent of shear on the iPP matrix directly in contact with the fiber could be created during the fiber introduction. If this is true, the produced column structures should be then referred as cylindrites according to the definition of Varga et al.[33] The dependence of β-iPP crystallization on the fiber introduction temperature can then be explained in the same way as the fiber-pulling test, where the β-crystallization of iPP occurs most easily at lower fiber pulling temperature and no β-crystallization of iPP takes place if the fiber is pulled at high temperatures, e.g., above 170 °C.[18,34]

According to the fiber pulling experiments, Varga et al. have proposed their first explanation for the mechanism of iPP β-crystallization.[18] On the basis of the existence of a thin α-iPP layers lain between the fibers, they argued that shearing the melt by fiber pulling yields primary α-row nuclei along the fiber. On the surface of these in situ formed α-row nuclei, a αβ growth transition takes place during crystallization process, which leads to the formation of a layer enriched in the β-phase of iPP along the pulled fiber. From the in situ rheo-X-ray results, Somani et al.[4] also suggested that the β-crystals could only grow after the formation of their oriented α-counterparts. The existence of α row nuclei in shear-induced crystallization has been proved by many optical microscopy and AFM observations.[18,33,35,36] Actually, the α row nuclei with β lamellar overgrowth was also observed during injection molding as proved inevitably by optical microscopy and SEM observation in the shear zone of

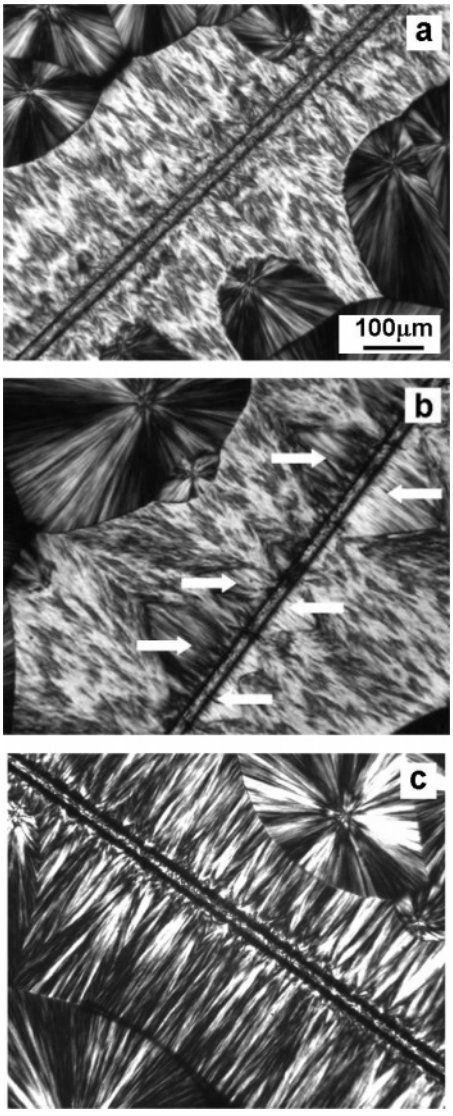

Figure 7. Optical micrographs of iPP/PET composites, which were prepared by introducing the PET fibers into the supercooled iPP melts at 145 °C. After fiber introduction, the samples were kept at 145 °C for (a) 5 s, (b) 30 s, and (c) 10 min and then cooled to 130 °C for isothermal crystallization.

the injection molded parts.[37] The smooth surface of the PET fiber after selective melting of the β-iPP crystals in our experiment, as shown in Figure 6b, indicates, however, the absence of the saw-toothed residual α-layer. One may argue that this is caused by the low resolution of optical microscope. To find out whether there is a very thin oriented α layer, an observation on lamellar level has been realized by scanning electron microscopy. Figure 8 shows a scanning electron micrograph of an iPP/PET sample prepared by introducing the PET fiber into the supercooled iPP melt at 140 °C and then crystallized isothermally at 130 °C for 90 min. The PET fiber was detached from the sample during etching (which is most likely dissolved by the etching agent), but the contour recording its original place (left part of the picture) can be recognized with careful inspection. From Figure 8, we see some small domains along the fiber as indicated by white arrows, which exhibit different contrast from the predominant β-iPP crystals and should be related to the α-form iPP crystals. These crystals cannot be revealed under optical microscope owing to their small size. The β lamellae are seen preferentially edge-on arranged perpendicular or approximately perpendicular to the fiber axis. However, there are flat on β lamellae with screw dislocations

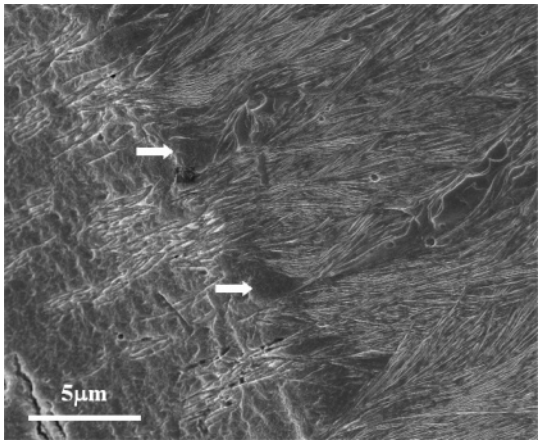

Figure 8. Scanning electron micrograph of an iPP/PET sample prepared by introducing the PET fiber into the supercooled iPP melt at 140 °C and then crystallizing the sample at 130 °C isothermally for 90 min. The PET fiber was detached away from the sample during etching.

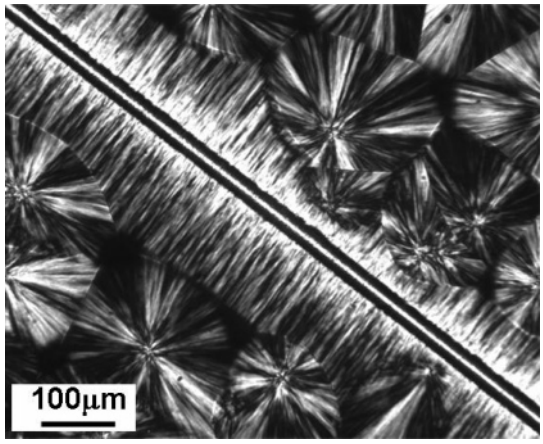

Figure 9. Optical micrograph shows the interfacial morphology of the iPP fiber/matrix single polymer composite prepared in the same way as that shown in Figure 7a.

on their surface on the right side (see the middle part) of the micrographs as well. This is in agreement with the observation of Varga et al.[20,38] Moreover, one can see parallel arranged β-iPP crystalline lamellae perpendicular to the fiber axis formed underneath the PET fiber, indicating a parallel alignment of iPP chains along the fiber axis. These structures have a close resemblance with the morphology of axialites, which is confirmed to form in the very early stage of β-crystal growth.[38] The out spreading of the β-iPP lamellae from these parts into the cylindrite indeed confirms that the β-iPP crystallization begins at these areas and ruled out the existence of a thin α layer between the PET fiber and the β-iPP cylindrite. This implies that the oriented α-iPP row nuclei are not the prerequisite for producing β-crystallization of iPP in the present case and seems contrary to the findings of Varga et al.[18] The fact that iPP chains aligned parallel to the fiber axis observed by SEM indicates that the observed supermolecular structures are actually not shear induced by fiber introduction. In our experimental procedure, the frame with fibers moves perpendicular to the plane of the molten film during the fiber introduction. In this case, the expected chain orientation should be perpendicular to the plan of the film or at least perpendicular to fiber axis. Moreover, the observed inhomogeneity of the structure along the fiber can also not be attributed to the orientation of chain segments. On the basis of the above analysis, there should be another factor controlling the formation of β-iPP structure.

As mentioned in the Introduction, crystallization of iPP in temperature gradient also encourages the crystallization of it in its β-phase.[24−26] It was reported that during crystallization in temperature gradient a kinetically favored α to β growth transition occurs owing to either the presence of latent β prenuclei or the influence of the local stresses.[19,25] In both cases, formation of α row nuclei is not necessary for the occurrence of α to β growth transition. The feature of the crystallization presented in here hints at the similarity with the crystallization in temperature gradient. Considering that the fiber is at room temperature before introduction and the difference in thermal conductivity of different materials, it is possible to produce a local temperature gradient during the experimental procedure. This kind of temperature gradient should be reduced (i) when the fiber is introduced at higher temperature for that a long time is needed to cool the sample to crystallization temperature and/or (ii) if the sample is kept at fiber introduction temperature for certain period of time before isothermal crystallization since equilibrium will be reached. In this case, the observed supermolecular structure can be understood. As for the different crystallization behavior of iPP at the tips and middle part of PET fiber, it is not clear now. Further investigation on this issue is undergoing.

Another thing to be addressed is the diverse outcome between the heterogeneity and homogeneity fiber/matrix systems.[27−29] For a direct comparison with most probably the same experimental condition, Figure 9 shows an optical micrograph of an iPP matrix/fiber homogeneity system, which was prepared by introducing the iPP fiber into its supercooled single polymer melt at 145 °C and then quickly crystallized isothermally at 130 °C for 90 min. Clearly, α-iPP cylindrite is the observed interfacial morphology. This demonstrates that although the experimental condition with iPP fiber is the same as that of PET fiber, the interfacial morphology of the single polymer composite is completely different from the iPP/PET system. While pure β-iPP cylindrites are generated in the iPP/PET system, iPP fiber initiates basically α-crystallization of its single polymer matrix. This seems unusual on the basis of the same experimental procedure. It rests in practice on different crystallization mechanisms. For iPP single polymer system, the existence of perfect lattice matching between the fiber and the single polymer matrix encourages the occurrence of polymer homoepitaxy, which is found to be quite efficient in improving the crystallization kinetics of a polymer.[39] Moreover, the better surface wettability of the iPP matrix on its own fiber will also enhance the adsorbability of iPP chains on the surface of the solid fiber and accelerate the secondary nucleation of the iPP chain on its homogeneity fiber. All of these enable a high nucleation ability of iPP fiber toward its homogeneity matrix. Our previous studies have also illustrated a very strong nucleation ability of solid iPP fiber toward its homogeneity matrix.[27,40] Taking all these into account, the homoepitaxial crystallization of iPP on the solid surface of its highly oriented single polymer fiber caused by heterogeneous nucleation (or secondary nucleation) is expected to overwhelm the effect of the fiber introduction. Therefore, transcrystallization of iPP in its α-form is generated since lattice matching possesses a very strong controlling power on the crystalline structure of the epitaxial polymer.[41−44] On the other hand, for the iPP/PET system, the PET fiber exhibits very weak capacity for nucleating iPP matrix as can be judged from the interfacial morphology produced in the quiescent condition (see Figure 10). In this case, the influence of fiber introduction procedure on the crystalliza-

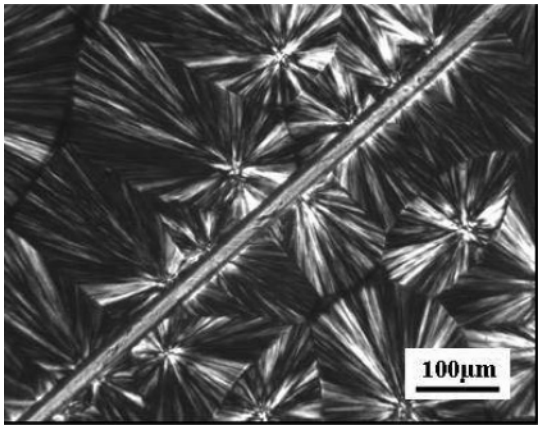

Figure 10. Optical micrograph showing the crystallization behavior of iPP on the surface of the PET fiber under quiescent conditions at 130 °C.

tion kinetics as well as the final morphology of iPP overwhelms the heterogeneous nucleation of iPP on the surface of the PET fiber. As a consequence, the resultant morphology is completely different from the crystallization of iPP in the iPP/PET composite under quiescent conditions, where the PET exerts only a moderate α nucleating effect toward iPP.[33,35]

Conclusion

Through introducing PET fibers into the iPP melt or supercooled melt, the iPP/PET matrix/fiber composite systems were prepared and the interfacial structures of the composites were studied by optical and scanning electron microscopies. The optical microscopy results indicate that the interfacial structure depends strongly on the fiber introduction temperature. It is found that at higher fiber introduction temperature, e.g., over 170 °C, the nucleation of iPP matrix is enhanced tremendously, but the crystallization of iPP takes place in its α-phase. At lower fiber introduction temperature, e.g., below 145 °C, the crystallization of iPP is completely in its *β*-phase. This is somewhat different from the iPP matrix/fiber single polymer composite, where homoepitaxy induced by highly oriented solid α-iPP fiber dominates the crystallization process of the iPP matrix and initiates the crystallization of iPP in its α-phase. It is also different from the crystallization of iPP in iPP/PET composite under quiescent conditions, where the PET exerts only a moderate α nucleating effect toward iPP. This may provide a new way for the preparation of *β*-iPP. Scanning electron microscopy results tell us that the *β*-iPP lamellar crystals grow directly from the surface of PET fiber with the iPP molecular chains parallel to the PET fiber axis. This implies that the *β* crystallization of iPP in the present case is not shear induced. The supermolecular structures of iPP/PET composites display the feature similar to the crystallization of iPP in temperature gradient. This could be in accordance with the complicated thermal program applied.

Acknowledgment. The financial support of the Outstanding Youth Fund, the National Natural Science Foundations of China (No. 50521302, 20423003, 20574079, 20634050, and 20604031), is gratefully acknowledged.

References and Notes

(1) Tribout, C.; Monasse, B.; Haudin, J. M. *Colloid Polym. Sci.* **1996**, *274*, 197.
(2) Nogales, A.; Hsiao, B. S.; Somani, R. H.; Srinivas, S.; Tsou, A. H.; Balta-Calleja, F. J.; Ezquerra, T. A. *Polymer* **2001**, *42*, 5247.
(3) Somani, R. H.; Hsiao, B. S.; Nogales, A.; Srinivas, S.; Tsou, A. H.; Sics, I.; Balta-Calleja, F. J.; Ezquerra, T. A. *Macromolecules* **2000**, *33*, 9385.
(4) Somani, R. H.; Hsiao, B. S.; Nogales, A.; Fruitwala, H.; Srinivas, S.; Tsou, A. H. *Macromolecules* **2001**, *34*, 5902.
(5) Somani, R. H.; Yang, L.; Hsiao, B. S. *Physica A* **2002**, *304*, 145.
(6) Somani, R. H.; Yang, L.; Hsiao, B. S.; Agarwal, P.; Fruitwala, H.; Tsou, A. H. *Macromolecules* **2002**, *35*, 9096.
(7) Agarwal, P. K.; Somani, R. H.; Weng, W.; Mehta, A.; Yang, L.; Ran, S.; Liu, L.; Hsiao, B. S. *Macromolecules* **2003**, *36*, 5226.
(8) Yang, L.; Somani, R. H.; Sics, I.; Hsiao, B. S.; Kolb, R.; Fruitwala, H.; Ong, C. *Macromolecules* **2004**, *37*, 4845.
(9) Somani, R. H.; Yang, L.; Hsiao, B. S.; Sun, T.; Pogodina, N. V.; Lustiger, A. *Macromolecules* **2005**, *38*, 1244.
(10) Kumaraswamy, G.; Kornfield, J. A.; Yeh, F.; Hsiao, B. S. *Macromolecules* **2002**, *35*, 1762.
(11) Seki, M.; Thurman, D. W.; Oberhauser, J. P.; Kornfield, J. A. *Macromolecules* **2002**, *35*, 2583.
(12) Pogodina, V.; Siddiquee, S. K. S.; VanEgmond, J. W.; Winter, H. H. *Macromolecules* **1999**, *32*, 1167.
(13) Pogodina, N. V.; Winter, H. H. *Macromolecules* **1998**, *31*, 8164.
(14) Kumaraswamy, G.; Varma, R. K.; Kornfield, J. A. *Rev. Sci. Instrum.* **1999**, *70*, 2097.
(15) Kumaraswamy, G.; Issaian, A. M.; Kornfield, J. A. *Macromolecules* **1999**, *32*, 7537.
(16) Leugering, H. J.; Kirsch, G. *Angew. Makromol. Chem.* **1973**, *33*, 17.
(17) Devaux, E.; Chabert, B. *Polym. Commun.* **1991**, *32*, 464.
(18) Varga, J.; Karger-Kocsis, J. *J. Polym. Sci., Part B: Polym. Phys.* **1996**, *34*, 657.
(19) Varga, J.; Ehrenstein, G. W. *Polymer* **1996**, *37*, 5959.
(20) Varga, J. *J. Macromol. Sci., Part B: Phys.* **2002**, *41*, 1121.
(21) Varga, J.; Karger-Kocsis, J. *Polymer* **1995**, *36*, 4877.
(22) Varga, J. *J. Mater. Sci.* **1992**, *27*, 2557.
(23) Varga, J.; Fujiwara, Y.; Ille, A. *Periodica Polytech. Chem. Eng.* **1990**, *34*, 255.
(24) Crissman, J. M. *J. Polym. Sci.* **1969**, *7* (A2), 389.
(25) Lovinger, A. J.; Chua, J. O.; Gryte, C. C. *J. Polym. Sci., Part B: Polym. Phys.* **1977**, *15*, 641.
(26) Fujiwara, Y. *Colloid Polym. Sci.*, **1975**, *253*, 273.
(27) Li, H.; Jiang, S.; Wang, J.; Wang, D.; Yan, S. *Macromolecules* **2003**, *36*, 2802.
(28) Sun, X.; Li, H.; Zhang, X.; Wang, J.; Wang, D.; Yan, S. *Macromolecules* **2006**, *39*, 1087.
(29) Li, H.; Zhang, X.; Duan, Y.; Wang, D.; Li, L.; Yan, S. *Polymer* **2004**, *45*, 8059.
(30) Li, H.; Liu, J.; Wang, D.; Yan, S. *Colloid Polym. Sci.* **2003**, *281*, 973.
(31) Sun, X.; Li, H.; Wang, J.; Yan, S. *Macromolecules* **2006**, *39*, 8720.
(32) Olley, R. H.; Bassett, D. C. *Polymer* **1982**, *23*, 1707.
(33) Varga, J.; Karger-Kocsis, J. *J. Mater. Sci., Lett.* **1994**, *13*, 1069.
(34) Wu, C.-M.; Chen, M.; Karger-kocsis, J. *Polymer* **1999**, *40*, 4195.
(35) Varga, J. Crystallization, Melting and Supermolecular Structure of Isotactic Polypropylene. In *Polypropylene: Structure, Blends and Composites*; Karger-Kocsis, J., Ed.; Chapman & Hall: London, 1995; Vol. 1, pp 56−115.
(36) Vancso, G. J.; Liu, G.; Karger-Kocsis, J.; Varga, J. *Colloid Polym. Sci.* **1997**, *275*, 181.
(37) Varga, J.; Mudra, I.; Ehrenstein, G. W. SPE, Inc. Technical Papers, XLIV; 1998, Vol. III, p 3492.
(38) Varga, J.; Ehrenstein, G. W. *Colloid Polym. Sci.* **1997**, *275*, 511.
(39) Liu, J.; Wang, J.; Li, H.; Shen, D.; Zhang, J.; Ozaki, Y.; Yan, S. *J. Phys. Chem. B* **2006**, *110*, 738.
(40) Li, H.; Zhang, X.; Kuang, X.; Wang, D.; Li, L.; Yan, S. *Macromolecules* **2004**, *37*, 2847.
(41) Lovinger, A. J. *Polymer* **1981**, *22*, 412.
(42) Wittmann, J. C.; Lotz, B. *Prog. Polym. Sci.* **1990**, *15*, 909.
(43) Kopp, S.; Wittmann, J. C.; Lotz, B. *Polymer* **1994**, *35*, 908.
(44) Kopp, S.; Wittmann, J. C.; Lotz, B. *Polymer* **1994**, *35*, 916.

MA071382X